

DANAE Letter of Intent

C. Biscari, D. Alesini, R. Bedogni, M.E. Biagini, R. Boni, M. Boscolo, B. Buonomo, M. Calvetti, M. Castellano, A. Clozza, G.O. Delle Monache, E. Di Pasquale, G. Di Pirro, A. Drago, A. Esposito, L. Falbo, A. Gallo, A. Ghigo, S. Guiducci, M. Incurvati, P. Iorio, C. Ligi, F. Marcellini, C. Marchetti, G. Mazzitelli, C. Milardi, L. Pellegrino, M.A. Preger, L. Quintieri, U. Rotundo, R. Ricci, C. Sanelli, M. Serio, F. Sgamma, B. Spataro, A. Stecchi, A. Stella, S. Tomassini, C. Vaccarezza, M. Zobov, *INFN-LNF, Frascati, Italy*

E.B.Levichev, N.A.Mezentsev, S.A.Nikitin, P.A.Piminov, D.N.Shatilov,
P.D.Vobly, *BNP, Novosibirsk, Russia*

B. Parker, *BNL, Brookhaven, USA*

J. Fox, D. Teytelman, *SLAC, Stanford, USA*

INTRODUCTION

Lepton factories based on double storage rings and high frequency collisions of flat beams were designed in the 1990s, and came to operation just before the end of last century. The Φ -factory in Italy, DAΦNE[1], and the two B-factories on opposite sides of the Pacific Ocean, KEKB[2] in Japan and PEP-II[3] in USA, are planning the end of their operations after almost one decade of operation. The community is waiting for the first beams of the new factories, BEPC-II[4], the Chinese tau-charm at Beijing, and VEPP-2000[5], the first collider based on round beam collisions, in Novosibirsk. The future upgrades after 2010 of the two B-factories and of the Phi-factory are the subjects of discussions in the flavour physics communities.

In Frascati the DAΦNE original physics program, ranging from K-physics, to nuclear and atomic physics, will be completed well before 2010, when the three experiments, KLOE[6], FINUDA[7] and DEAR[8], will collect the required statistics. Interest in pursuing further these research fields, together with a wider particle physics program, including γ - γ experiments, has shown up and is described in separated documents [9-12]. The proposed experiments at the Φ are more demanding in terms of luminosity with respect to the present DAΦNE parameters, and even the foreseen collider upgrades for the next future will not fulfill completely the experimental requirements. A flexible range of energy is furthermore requested, to cover the energy span in between the Φ and the tau-charm resonances.

This document describes the feasibility study of an e^+e^- collider whose range of energy and luminosity is shown in Table I. The design is site dependent since it is optimized to use DAΦNE buildings, infrastructures, injection system, and part of the ring hardware, with an overall minimization of cost and construction time.

Following the Frascati tradition of applying mythological names to its accelerators, we have called it DANAE (DAΦNE New with Adjustable Energy). Danaë, the daughter of the King of Argos, shut by her father in a tower with bronze doors, was visited by Zeus in the form of a shower of gold falling from a cloud, and from their union Perseus was born.

Table I – DANAE Luminosity and Energy Range

Energy in the center of mass (GeV)	1.02	2.4
Peak luminosity > ($\text{cm}^{-1}\text{sec}^{-2}$)	10^{33}	10^{32}
Total integrated luminosity (fbarn^{-1})	50	3

The project excellence is assured by the application of the most recent technologies, on the basis of experience from DAΦNE and the group expertise, and by the possibility of using the next DAΦNE runs as R&D for some of the proposed new principles.

The accelerator community has recently evolved towards a phase of extended collaborations in view of the construction of large projects, like ILC [13], thanks also to the ever increasing participation of the Asian world. Even small projects like DANAE take advantage of this new attitude and several international groups participate to the collider design.

DANAE design is the final step of a process in which the possibilities to upgrade DAΦNE in energy and/or luminosity have been investigated, a process which started in the workshop held in Alghero in September 2003 [14]. Let's summarize the conclusions reached so far:

- The maximum luminosity for a Φ -factory based on present knowledge, and involving a time limited R&D is in the range of $10^{33} \text{ cm}^{-2}\text{sec}^{-1}$. Luminosity higher by one order of magnitude can be envisaged if very innovative regimes are foreseen (such as the strong RF focusing [15]), needing strong R&D effort, and not risk free. Going to still higher values is not conceivable at present even with the most imaginative accelerator designs.
- The maximum energy reachable by the DAΦNE complex with the present hardware is 750 MeV per beam. By substituting dipoles, splitters and the Interaction Region, the energy of 1 GeV per beam can be reached, not yet satisfying the experimental requirements. A preliminary evaluation of the necessary changes to reach the energy of 1.2 GeV per beam [16] has shown that the vacuum chamber and part of the magnetic elements need to be substituted. The luminosity required at the neutron-antineutron form factor threshold is in the range of $10^{32} \text{ cm}^{-2}\text{sec}^{-1}$, and does not represent a major challenge for the design, but for the particle losses, which must be kept below the allowed radiation doses, if the LNF buildings are being reused.

Summing up all above considerations we came to the design of a flexible collider, with the luminosity optimized at the Φ energy, and with the maximum reachable energy compatible with the present LNF infrastructures. The design is flexible enough to ensure the possibility of future upgrades in view of further developments in the field of collider physics, but is based on well assessed principles, in order to shorten as far as possible the time necessary for its completion.

In the following the collider design is briefly described, while the estimated cost and schedule are shown in the final paragraph.

DESIGN CRITERIA

The most demanding set of DANAE parameters corresponds to the high luminosity at the Φ -energy. The luminosity at higher energy comes almost for free once the collider hardware is correctly dimensioned.

The basic DANAE design criteria are the same adopted by all factories up to now: double ring, multibunch regime, flat beams and high collision frequency.

All factories run with a single experiment in the machine: the present DAΦNE layout has two Interaction Regions (IRs), where two experiments can be installed at the same time, but only one takes data while the other one is parked. In fact the optimization of the luminosity parameters in two collision points and background shielding on both IRs has shown to be critical, and it is more effective in terms of peak and integrated luminosity to dedicate each run to a single detector.

DANAE has therefore one single IR, where the experiments will be installed sequentially, thus leaving a long straight section opposite to the IR free, which can be used for injection, RF and feedback systems.

If the different experiments use a single detector, gain in shutdown and commissioning time is obtained. The DANAE design is based on the reutilization of the KLOE detector, with a tunable IR fitting different energies and detector solenoid field.

One of the main characteristics of the new collider is its flexibility. Beyond the two nominal sets of parameters, one corresponding to the high luminosity in the regime of Φ -factory, the second to the maximum reachable energy, the possibility of tuning the main collider parameters in a wide range is kept, with special care to the tunability of momentum compaction, emittance and betatron tunes. All quadrupoles and sextupoles will have independent power supplies following the DAΦNE approach which has proven to be very useful during machine commissioning, machine study shifts and operation.

Table II contains the list of the main parameters for the two operating conditions, compared to those of DAΦNE corresponding to the peak luminosity reached so far.

It can be remarked that the gain in luminosity with respect to the present DAΦNE parameters is based on the increase of collision frequency, thanks to the higher RF frequency, of the colliding currents, but specially of the specific luminosity.

Let's recall the luminosity expression:

$$L = \frac{f_{coll}}{2\pi} \frac{N^+ N^-}{\Sigma_x^* \Sigma_y^*} \quad (1)$$

where

$$f_{coll} = N_b f_o \quad (2)$$

is the collision frequency, defined by the number of bunches N_b and the revolution frequency f_o ; N^+ and N^- are the number of particles per bunch and

$$\Sigma_{x,y}^* = \sqrt{\sigma_{+,x,y}^{*2} + \sigma_{-,x,y}^{*2}} \quad (3)$$

are the beam cross sections at the Interaction Point (IP).

Table II – DANAE design parameters as a Φ -factory and at the maximum energy, compared with DAΦNE parameters at the present peak luminosity.

		Units	DAΦNE	DANAE @ Φ	DANAE 1.2 GeV
Date			2006	16-3-2006	16-3-2006
Energy (center of mass)	E_{cm}	GeV	1.02	1.02	2.4
Energy per ring	E	GeV	0.51	0.51	1.2
Number of rings			2	2	2
Circumference	C	m	97.69	96.34	96.34
Number of IPs			1	1	1
Revolution frequency	f_{rev}	MHz	3.07	3.11	3.11
Time between collisions	T_c	nsec	2.7	2.0	6.0
Bunch spacing	s_b	m	0.81	0.60	1.80
Half crossing angle	$\theta/2$	mrad	15	15	15
# of Colliding Bunches	N_b		110	150	30
Particles per bunch	N_{part}	(10^{10})	2-3	3	3.4
Beam current (e-/e+)	I	A	1.4/1.3	2.25	0.5
Bunch current (e-/e+)	I_b	mA	13/12	15	16.6
Peak Luminosity (10^{32})	L_{peak}	$cm^{-2}sec^{-1}$	1.5	10	> 2
Specific Luminosity/bunch (10^{28})	L_{sp}	$cm^{-2}sec^{-1}mA^{-2}$	0.9	3	3
Horizontal β function @ IP	H	m	2	1	1
Vertical β function @ IP	V	cm	1.8	0.8	1
Horizontal emittance	ϵ	mm mrad	0.4	0.45	0.45
Coupling factor	κ	%	1.1	0.5	0.5
Horizontal Σ in collision	Σ_x	mm	1.26	0.95	0.95
Vertical Σ in collision	Σ_y	μm	12.6	6	6.7
Horizontal Beam-beam tune shift	ξ_x		0.026	0.030	0.014
Vertical Beam-beam tune shift	ξ_y		0.025	0.038	0.020
Bunch length (e-/e+)	σ_L	cm	3/2	1	1.5
Piwinski angle*	ϕ		0.42	0.22	.33
Momentum compaction	α_c		0.027	0.02	0.03
Synchrotron radiation integral	I_2	m^{-1}	9.5	22.4	5.6
Synchrotron radiation integral	I_3	m^{-2}	8.5	42.6	3.6
Synchrotron radiation integral	I_4	m^{-1}	0.3	0.2	0.5
Synchrotron radiation integral	I_5	m^{-1}	9.6	23.9	1.1
Energy loss per turn	U_0	keV	9	21.4	165
Longitudinal damping time	τ_s	msec	17.9	7.6	2.2
RF frequency	f_{rf}	MHz	368.26	500	500
RF voltage (e-/e+)	V	MV	0.12/0.18	0.4	1.5
Ring impedance	Z/n	Ω	1.1/0.6	0.5	0.5
Total Beam Power	P_t	kW	45**	48	83
Wiggler beam power	P_w	kW	24**	42	43
Dipole beam power	P_d	kW	21**	6	40
Injection energy	E_{inj}	GeV	0.51	0.51	0.51

* The Piwinski angle is defined as: $\phi = \theta \sigma_L / 2\sigma_x$

** These values refer to DAΦNE design for a maximum current of 5A per beam

The so called specific luminosity per bunch is defined as

$$L_{sp} = \frac{L_{bunch}}{I_b^+ I_b^-} \quad (4)$$

Keeping the beam cross section small in collision at high currents is the key point of the high luminosity regime. Let's now mention briefly the considerations on which we base our nominal set of parameters.

In a flat beam collider the beam size at the IP is minimized by the smallest achievable vertical β^* compatible with chromaticity contribution and especially with bunch length: the bunch length should be comparable or slightly longer than β^* , otherwise the luminosity decreases very fast due to the geometric "hourglass effect" and beam-beam synchrotron resonances.

The bunch design current should not exceed too much the threshold current of the longitudinal microwave instability in order to avoid the drawbacks which appear above the threshold. The MI threshold is given by [17]:

$$I_{th} = \sqrt{2\pi} \frac{\alpha_c (E/e) (\sigma_E/E)^2 \sigma_l}{|Z/n|R} \quad (5)$$

where the natural energy spread is:

$$\frac{\sigma_E^2}{E^2} = C_q \gamma^2 \frac{I_3}{I_2 + I_4} \quad (6)$$

with $C_q = \frac{55}{32\sqrt{3}} \frac{hc}{2\pi mc^2} = 3.8319 \cdot 10^{-13} m$

I_j are the synchrotron radiation integrals [18] and $Z_{||}/n$ is the ring impedance.

The first phenomenon is the bunch length and energy spread growing with the product of the bunch current and the ring impedance. A correlated vertical size blow up has also been observed at DAΦNE [19].

Other effects are the coherent oscillations inside the bunch like the "saw-tooth" oscillations seen at SLAC damping ring [20] or the "quadrupole mode instability" in the DAΦNE electron ring [21]. Such oscillations in collisions lead to beam lifetime reduction, luminosity decrease and excessive background in the detector.

It is clear that the impedance minimization of all elements of the vacuum chamber is of extreme importance, both to increase I_{th} and to decrease the strength of the instability. Experience in the DAΦNE vacuum chamber design, which has obtained the minimum ring impedance for such short machines (0.6 Ω for the positron ring and twice as much for the electron one, the difference due to the presence of long ion clearing electrodes, ICE) will be of great help.

The longitudinal synchrotron tune Q_s should not be too high. This has been confirmed by the dedicated measurements at CESR of the luminosity versus the synchrotron tune [22] and has been also verified in numerical simulations of the beam-beam effects for DANAE.

The emittance is chosen by finding the best compromise between two different effects: a high value is positive from the point of view of beam-beam tune shift, a low one is better from the point of view of parasitic crossings and small cross section at collision.

The radiation damping increase is beneficial for several reasons, first of all the shorter damping time, which interferes with the beam-beam behavior and with all instabilities with risetimes in the range of msec, including the injection procedure, as shown recently in CESR-c operation at low energy [22]. A second advantage, if the wigglers increase the synchrotron radiation integral I_3 more than I_2 , is that the ring will have a larger natural energy spread, and therefore the value of I_{th} will be increased. On the other hand, a drawback introduced by the wigglers can be the effect of non-linearities on dynamic aperture and beam-beam behavior. Wigglers placed in regions with low dispersion and low beta values are less harmful.

The possibility of realizing a lattice with negative momentum compaction is included in the design. Negative α_c regimes correspond to shorter bunches, but lower I_{th} . [23]

The linear beam-beam tune shift neglecting crossing angle and hourglass effect is:

$$\begin{aligned}\xi_x &= \frac{r_e}{2\pi\gamma} \frac{N}{\epsilon_x} \\ \xi_y &= \xi_x \sqrt{\frac{\beta_y^*}{\kappa\beta_x^*}}\end{aligned}\tag{7}$$

The luminosity can be written in terms of the beam-beam tune shifts:

$$L_{bunch} = f_o \frac{\pi\gamma^2}{r_e^2} \xi_x \xi_y \frac{\epsilon_x}{\beta_y^*}\tag{8}$$

The choice of emittance, horizontal and vertical β^* and coupling factor determines the beam-beam tune shift and the luminosity. We remark again the importance of maintaining the flexibility of choosing different sets of parameters in order to explore during collider operation the most effective regimes to increase the luminosity. Table III shows the tuning range of the most significant among them.

The approach to high currents is based on a careful design of all impedance creating elements in the ring, specially the RF cavity, and on the optimization of the feedback systems, as a natural evolution of the experience gained on DAΦNE. For the e- ring, ion trapping will be avoided by using small ICE made of Alumina coated with a thin layer of highly resistive material distributed along the ring, with a very small impedance contribution, and by filling the ring with a gap in the bunch train, while Ti coating and antechambers in the positron ring will fight the electron cloud instability.

The injection efficiency will be optimized by doubling the injection transfer lines in order to eliminate the time needed for switching between e^+ and e^- injection configurations.

The DANAE energy range goes from 0.5 to 1.2 GeV per ring. The maximum current at the maximum energy is limited to 0.5 A, in order to keep the total beam power within reasonable limits.

Injection is kept at low energy, so that the injection system does not need major modifications, and radiation shielding at injection is less demanding. Rings will be filled up to the operating current, and then ramped together up to the maximum energy.

Table III – Range of tunability of specific parameters for Φ operation. For each parameter the minimum and maximum values are given; the two columns do not represent a coherent set of parameters.

Parameter	Symbol	Units	Min	Max
Emittance	ϵ_x	mm mrad	0.2	0.5
Momentum compaction	α_c		-0.03	0.05
Horizontal β^*	β_x^*	m	0.5	1.5
Vertical β^*	β_y^*	mm	5	10
Coupling	κ	%	0.3	1
Half horizontal crossing angle	θ_{cross}	mrad	10	20
Number of particles per bunch	N	10^{10}	2.8	4
Bunch current	I_{bunch}	mA	13.8	20
Total current	I_{tot}	A	2	3
rf voltage	V	MV	0.4	1.5
Bunch length	σ_L	mm	8	15
beam-beam tune shift	$\xi_{x,y}^*$		0.025	0.06
Synchrotron tune	Q_s		0.02	0.10

Further upgrades

The basic DANAE design is based on already well assessed principles, on the present knowledge in collider physics, and especially on experience from DAΦNE. It includes however the possibility of adding new features, in order to open in the future other possibilities for increasing the luminosity.

One of these is the installation of *crab cavities*, which are beneficial to the beam-beam behavior, because they transform the collision with crossing angle into a head-on-like ones.

The long straight section opposite to the IR has available space for such a device, and the flexibility of the optics allows tuning the lattice for such a regime. Let's recall that the effectiveness of such devices will be tested in few months by the KEKB team on their B-factory, since in the present shutdown they are installing one crab cavity per ring [24].

Also the *Strong RF focusing* regime [15] could be implemented: the modulation of the bunch length allowing values of the vertical betatron function at the IP in the range of very few mm can be obtained by a regime with high RF voltage derivative and large dispersion in the dipoles, producing a drift of the longitudinal phase plane along the orbit. The regime in which the drift changes sign in the two arcs of the ring, corresponding to a small momentum compaction, can be applied to DANAE, with the high voltage cavity placed in a zone near the IR, in order to have the minimum bunch length at the IP. The necessary space for the harmonic cavity yielding the strong RF focusing is in fact foreseen in the ring layout.

COLLIDER DESIGN

Lattice design

The lattice of a Φ -factory based on a multibunch double ring with flat colliding beams is of course an evolution of the present DAΦNE design, with the modifications dictated by the past experience and the new available technology.

The ring layout consists of one IR, two arcs, the long and the short ones, and a long straight section opposite to the IR housing injection, RF and feedback systems. The two rings cross only at the Interaction Point (IP), while on the opposite point the two vacuum chambers are vertically separated avoiding parasitic crossings. In the central part of each arc there is a superconducting wiggler, to increase radiation and shorten damping times.

Emittance and momentum compaction can be tuned by varying dispersion and betatron functions in both arcs. The beams enter the IR from the long arc, and the section between the long arc and the IR is optimised to minimize the background induced inside the detector by particles scattered in the last dipole, while the rest of the background is shielded along the ring by a scraper system.

Figure 1 shows the layout of the rings inside the DAΦNE hall. The IR is centered in the same position as the present IR1 of DAΦNE, in order to reuse the existing KLOE detector infrastructures. Gray lines indicate the present DAΦNE rings, red and blue correspond to DANAE e^+ and e^- rings and new transfer lines.

The Interaction Region (IR) design fits different energies and solenoid fields and is compatible with the KLOE detector.

The low-beta quadrupoles are based on the superconducting technology which is being developed for ILC [25], has been already successfully tested in HERA and CESRc and is being installed in BEPCII rings. The quadrupoles include skew and dipole coils, thus avoiding the mechanical rotation of quadrupoles and allowing closed orbit correction; the same technology provides the antisolenoid placed inside the detector [26]. Figure 2 shows a sketch of the IR layout.

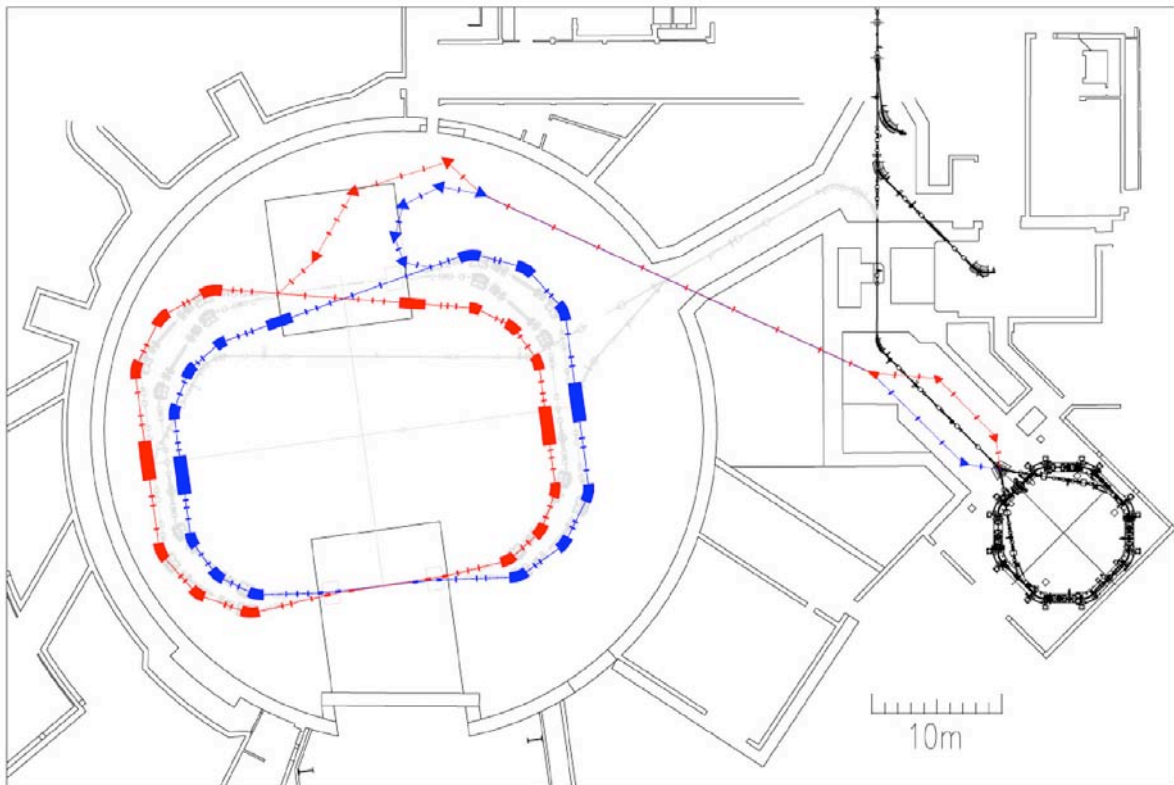


Figure 1 – Layout of DANAE inside the DAΦNE hall. Blue (red) lines correspond to e^- (e^+).

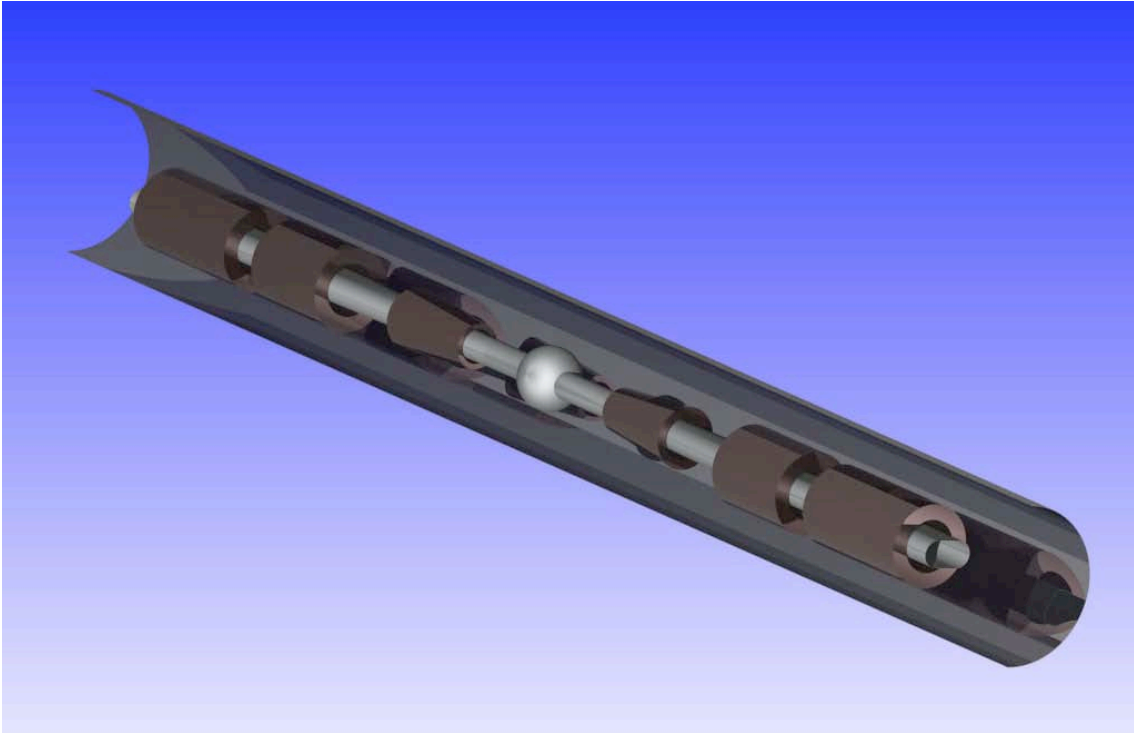


Figure 2 – Interaction Region 3D schematic design, showing quadrupole and antisolensoid positions on both sides of the present KLOE IR vacuum chamber.

Beams cross at a horizontal angle of 30 mrad providing the necessary separation at the first parasitic crossing for the Φ operation, where the distance between bunches is very small. The IR lattice is based on low-beta doublets, and the antisolensoid is placed just after the two quads, so that the coupling is corrected inside the detector. The vacuum chamber is common for the two beams in the detector zone, and splits just at the detector ends. Two downstream dipoles increase the separation between the beams. Figure 3 shows the horizontal and vertical trajectories in half IR for the Φ -energy, together with the beam stay clear, computed as $10 \sigma_x, \sigma_y$.

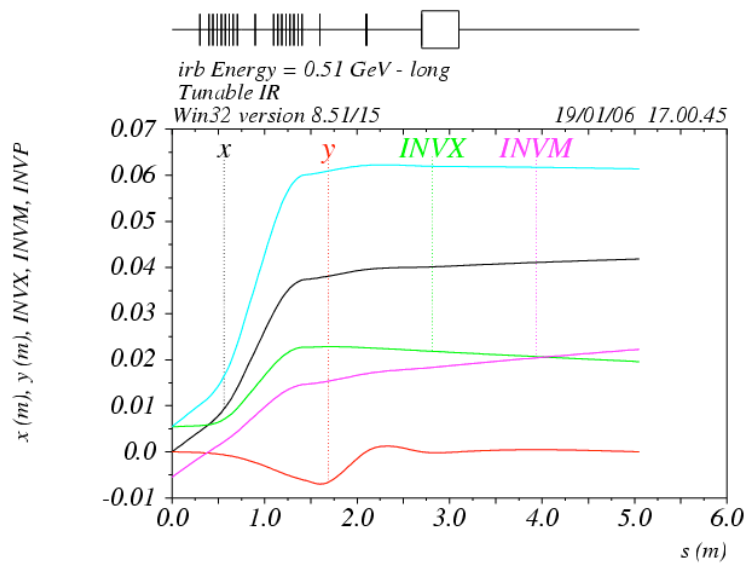


Figure 3 – Horizontal beam separation and beam stay clear in m for $E = 0.51$ GeV.

Betatron and dispersion functions along the whole ring, for the two operating energies, are shown respectively in Figs. 4 and 5, starting from the Interaction Point (IP).

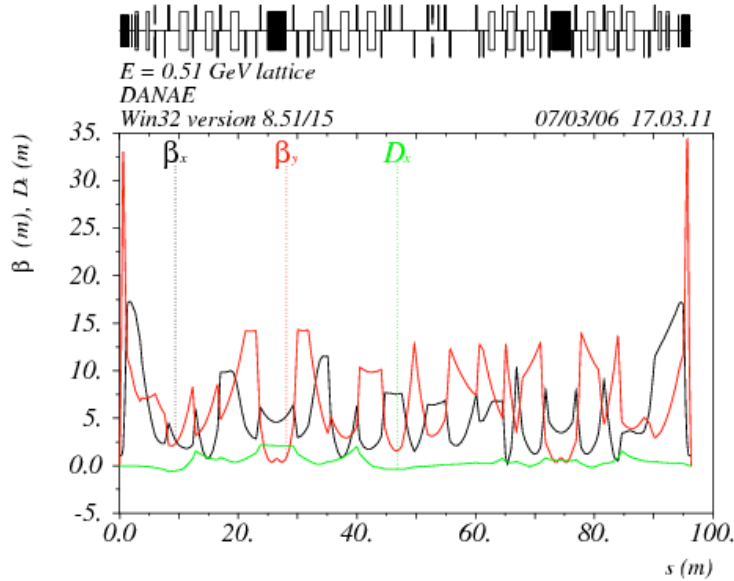


Figure 4 – DANA E Optical functions for the Φ -factory.

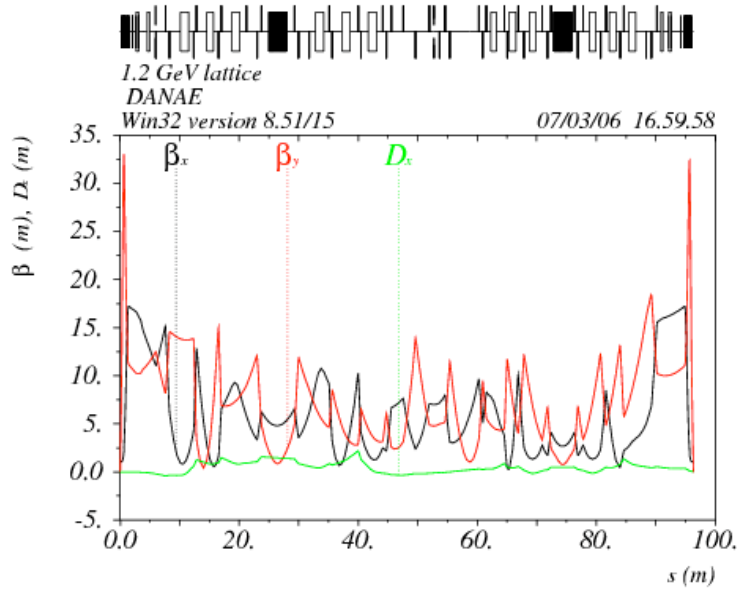


Figure 5 – DANA E optical functions for 1.2 GeV operation.

The dipoles are normal conducting ones, with a maximum field of 1.72 T at the maximum energy and 2.3 m bending radius. The dipole contribution to the damping is weak

$$I_{2,dip} = \frac{2\pi}{\rho_{dip}} = 2.74 m^{-1}$$

and the presence of superconducting wigglers adds the necessary damping. In a wiggler the value of I_2 depends only on B_{max} and on the total length. Our nominal parameters

correspond to $B_{\max} = 4\text{T}$ for a total length of 6m per ring. The wigglers modify also the synchrotron integral I_3 , which determines the natural energy spread and therefore the microwave instability threshold which depends quadratically on it. The choice of the pole length is led by the optimization of the nonlinear terms. For a given energy the trajectory oscillation amplitude depends quadratically on the pole length and linearly on the peak magnetic field. For a high magnetic field it is convenient to shorten the pole length in order to reduce the required transverse good field region, down to the value where the increase of the pseudo-octupole term, coming from the longitudinal drop of the field between poles becomes too harmful for the beam dynamics.

The values chosen for the design are summarized in Table IV. CESR-c wiggler design [22] has been followed for the choice of the number of poles: an even number of poles corresponds to a trajectory oscillating around the wiggler axis for any energy and/or any magnetic field value, and it is particularly convenient for a collider running under different operational conditions.

Figure 6 shows the magnetic field longitudinal distribution.

Table IV – SC wiggler characteristics

Energy		0.51	1.2
Maximum magnetic field B_{\max}	T	4	4
Total number of poles		19	19
Total length	m	2.96	2.96
Central pole length	cm	16	16
End poles length	cm	8	8
2 nd and second-last poles length	cm	12	12
End poles field ratio to B_{\max}		0.5	0.5
2 nd and second-last field ratio to B_{\max}		1	1
Max trajectory oscillation	mm	6	2.5
Path – wiggler length difference	mm	11.8	2.1
Total vertical beam stay clear	cm	2	2
Total horizontal beam stay clear	cm	8.5	8.5

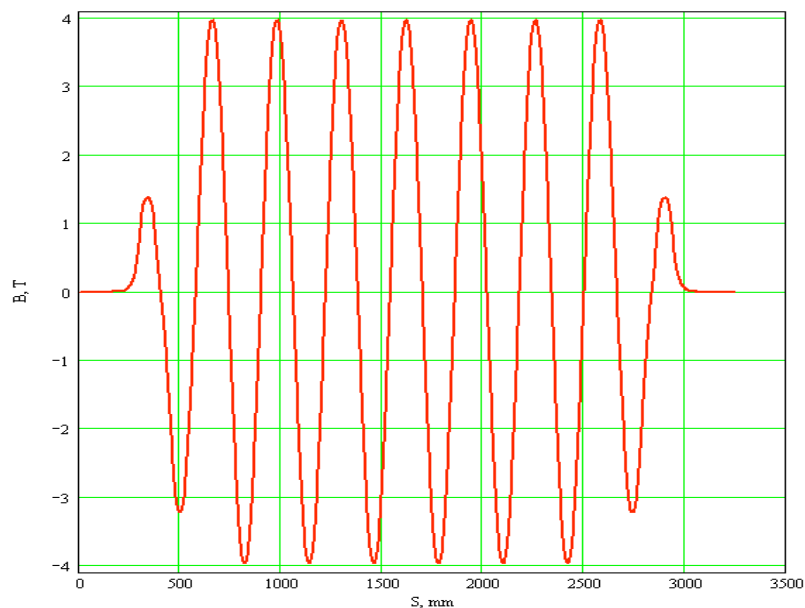


Figure 6 –Magnetic field distribution in the wiggler.

Beam dynamics simulations

The Φ -factory regime has been investigated more in detail and in the following the different beam dynamic simulations refer to the low energy case. All items are much less demanding for the case of high energy, and will not be mentioned in this paragraph.

Dynamic aperture

A large dynamic aperture is one of the essential characteristics of the Φ -factory both for the beam lifetime and the beam-beam behavior.

A first optimization of the dynamic aperture has been performed for the nominal lattice and the nominal tunes with no errors nor multipole components.

The sextupole configuration has been optimized by correcting to zero the natural chromaticity of the lattice. Table V shows the main parameters used for the tracking calculations and the results for the dynamic aperture in terms of the bunch sizes.

Table V – Parameters used in the tracking calculations and dynamic aperture results.

	Horizontal	Vertical
Betatron tunes	5.15	5.21
Natural chromaticity	-10	-19
Corrected chromaticity	0	0
DA on energy	$25 \sigma_x$	$300 \sigma_y$
DA off energy (0.5%)	$17 \sigma_x$	$230 \sigma_y$
DA off energy (1%)	$9 \sigma_x$	$120 \sigma_y$

Let's remark that the natural chromaticity is lower than the present DA Φ NE one, even if the low beta value is smaller, since special care has been used in the linear design to minimize the chromaticity contributions in the whole ring.

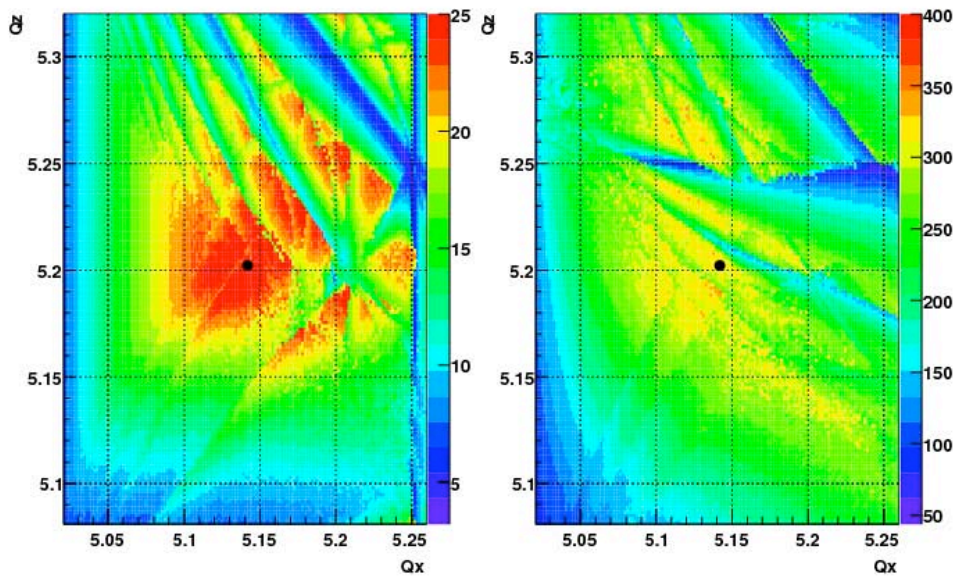


Figure 7 – Horizontal (left) and vertical (right) dynamic aperture betatron tune scans.

A total number of 15 sextupole families have been used. The results are satisfactory: on energy the stable region is larger than $20 \sigma_x$ and $300 \sigma_y$ at the nominal coupling, and for the best configuration the off-energy dynamic aperture at 1% energy deviation (corresponding to $17 \sigma_p$) is still $10 \sigma_x$ and $100 \sigma_y$. With the best configuration a tune scan has been performed and the results are shown in Fig. 7.

Even if these results are already satisfactory, further optimization is foreseen in the future to explore the tune regions preferred by the beam-beam behavior, which stay closer to the integer, as shown in the next paragraph.

Beam-beam

In order to estimate the luminosity that can be obtained with the design parameters and to find the working points where the maximum luminosity can be achieved we have performed beam-beam simulations with the BBC code. The code simulates weak-strong beam-beam interaction in the 6D phase space including all principal effects influencing the luminosity: finite crossing angle, hourglass effect, longitudinal beam-beam kick etc.

The main parameters used in the simulations are listed in Table VI. Note that the bunch length at the nominal bunch current of 15 mA is 10 mm for positive momentum compaction ($\alpha_c=+0.02$) and 8 mm for negative ($\alpha_c=-0.03$), as given by the longitudinal dynamics modeling that takes into account bunch lengthening due to vacuum chamber wake fields.

Table VI – Beam parameters used for beam-beam simulations

Emittance	$\epsilon_x = 0.45 \times 10^{-6} \text{ m rad}$
Coupling	$k = 0.3\%$
Horizontal beta	$\beta_x = 1.2 \text{ m}$
Vertical beta	$\beta_y = 8 \text{ mm}$
Energy spread	$\sigma_E/E = 5.4 \times 10^{-4}$
Number of particles	$N = 3 \times 10^{10}$
RF frequency	$f = 500 \text{ MHz}$
RF voltage	$V = 400 \text{ kV}$
Half crossing angle	$\phi = 15 \text{ mrad}$
Momentum compaction	$\alpha_c = +0.02; -0.03$

In order to find suitable working points we have carried out luminosity scans in the tune diagram area $Q_x = (0.05-0.15)$, $Q_y = (0.05-0.15)$. We have chosen these tune intervals for our study since the area above the integer is well suited for low energy colliders like ADONE, VEPP-2M and DAΦNE. In particular, the maximum single bunch luminosity of $5 \times 10^{30} \text{ cm}^{-2} \text{ s}^{-1}$ at the Φ -resonance was obtained by VEPP-2M at the tune $\sim (0.06, 0.10)$ [27].

The tune scan (contour plot) performed for positive momentum compaction is shown in Fig. 8 on the left. The brighter red colors correspond to the higher luminosity while the green-yellow-brown ones indicate the strongest luminosity reduction (typically on beam-beam resonances). The maximum attainable peak luminosity is close to $10^{33} \text{ cm}^{-2} \text{ s}^{-1}$, and is achieved at the tunes in the red area, near the point (0.06, 0.12). In turn, a luminosity around $9 \times 10^{32} \text{ cm}^{-2} \text{ s}^{-1}$ can be obtained inside the magenta contours. Nevertheless the practical realization of these luminosity values is not simple since the safe tune area is small, the good working points are very close to the horizontal integer, where the dynamic aperture is intrinsically lower, and to the skew sextupole resonance $2Q_x = Q_y$ which can be dangerous both for the lifetime and for coupling correction.

The situation is much better if we exploit a lattice with negative momentum compaction (see Fig. 8 - right). In that case a luminosity of $1.2 \times 10^{33} \text{ cm}^{-2} \text{ s}^{-1}$ can be obtained at the three working points: (0.06, 0.11), (0.05, 0.09) and (0.10, 0.06). Moreover, the tune area where luminosity above $10^{33} \text{ cm}^{-2} \text{ s}^{-1}$ is reachable is definitely much wider (see the violet contour areas).

Crab-cavities can improve the luminosity further (see Fig. 9). By comparing Figs. 8 and 9 one can see that the beam-beam resonances $2Q_x = Q_y$ induced by the finite crossing angle are eliminated in the crab-crossing scheme. The good “safe” areas become larger and, in principle, further luminosity increase is possible for higher (than design) bunch currents.

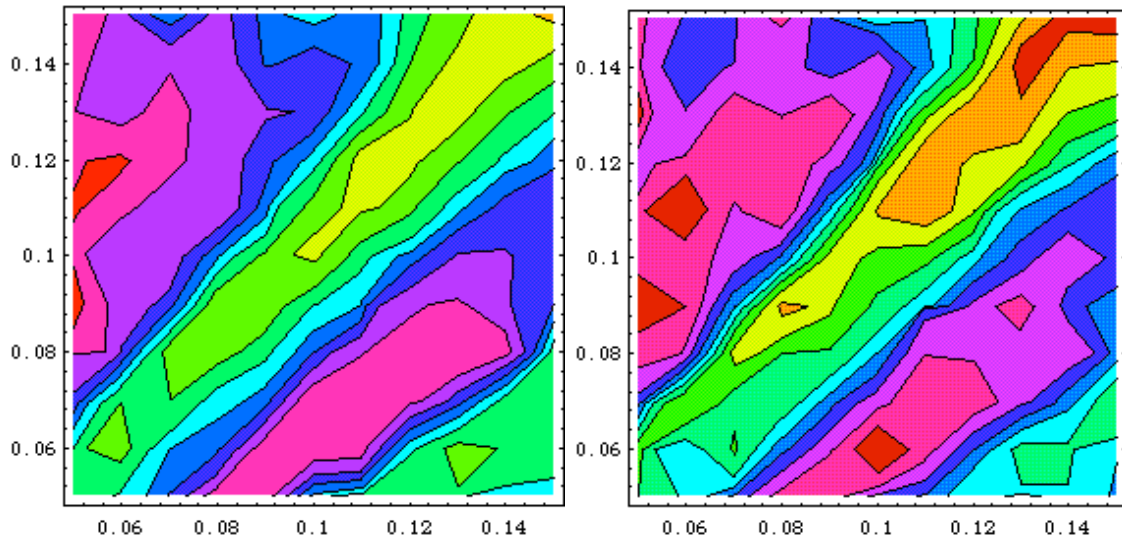


Figure 8 – Beam-beam simulations for positive and negative momentum compaction regimes at low energy.

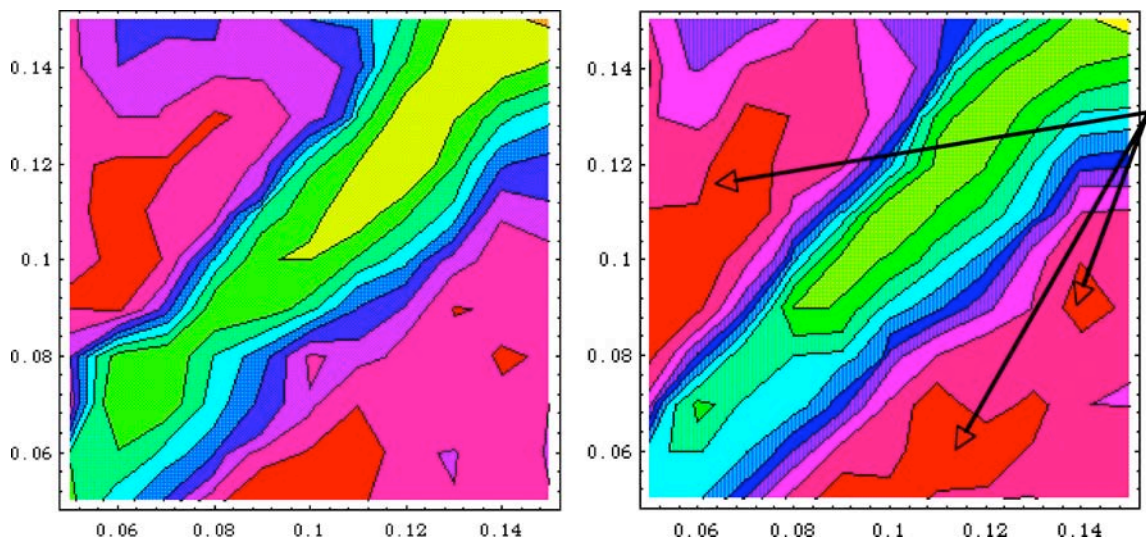


Figure 9 - Beam-beam simulations for positive and negative momentum compaction regimes at low energy with crab-crossing.

Bunch lengthening

In order to choose the parameters affecting the longitudinal dynamics a series of numerical simulations of the bunch lengthening in DANAE have been performed. They are based on the longitudinal wake fields calculated for the DAΦNE positron ring which proved to reproduce very well not only the bunch lengthening but also the internal motion in the positron ring bunches [28]. This is a reasonable, even conservative, approach since many DAΦNE vacuum chamber components will be reused in DANAE, and furthermore we expect to improve the DANAE beam coupling impedance with respect to that of DAΦNE.

The final results satisfying above requirements are presented in Figs. 10-14. In particular, as it can be seen in Fig. 10, with 400 KV RF voltage and positive momentum compaction ($\alpha_c = 0.02$) the bunch length at the design bunch current of 15 mA (3×10^{10} particles per bunch) is 10 mm (to be compared to 8-9 mm vertical beta function at the IP).

The threshold current for these parameters is higher than the design value. The threshold at about 20 mA is clearly seen in Fig. 11: it corresponds to the point where the bunch energy spread starts growing.

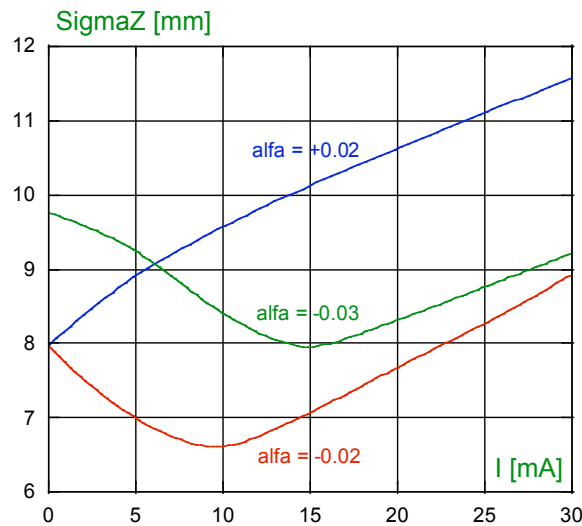


Figure 10 - Bunch lengthening versus bunch current.

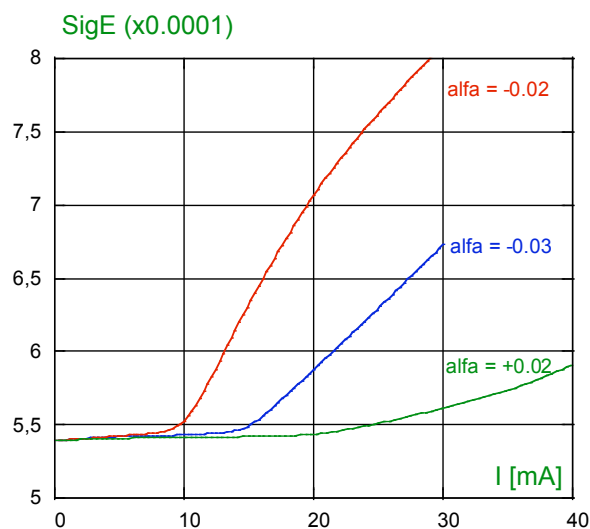


Figure 11 - Bunch energy spread versus bunch current.

Even shorter bunches can be obtained at the design current by using a lattice with negative momentum compaction. In this case the bunch shortens until the microwave instability threshold is reached. As one can see in Fig. 10 and Fig. 11, with $\alpha_c = -0.03$ the bunch at 15 mA is focused by the wake fields down to 8 mm without energy spread growth. It is also possible to obtain a shorter bunch length with a negative momentum compaction having lower absolute value. However, in such cases the design current becomes higher than the microwave instability threshold (see the plots for $\alpha_c = 0.02$, as an example).

The resulting bunch shapes for positive (+ 0.02) and negative (- 0.03) momentum compaction factors are shown in Fig. 12, while the corresponding bunch distribution centroid shifts with current are plotted in Fig. 13.

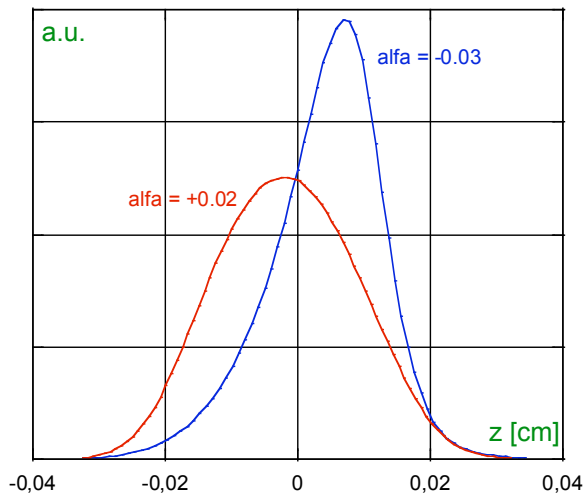


Figure 12 – Bunch shape for positive (red) and negative (blue) momentum compaction factors.

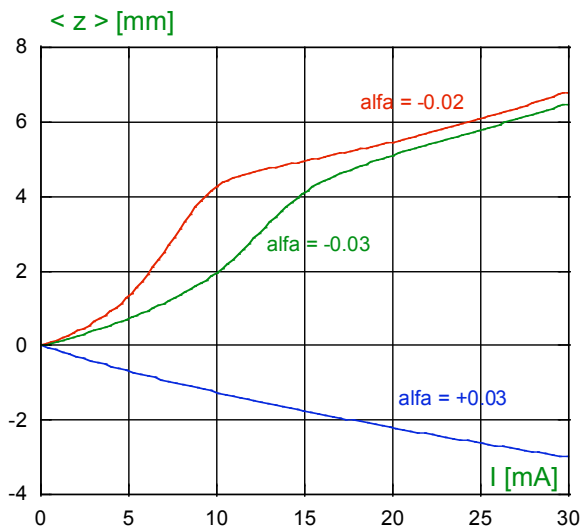


Figure 13 – Bunch distribution centroid shift versus bunch current.

Touschek lifetime

The beam lifetime has been calculated taking into account the intrabeam scattering processes. With the aim to clarify the role of the localized betatron coupling correction over the IR, the calculation is performed with and without the IR contribution. Figure 14 shows BLT (Beam Life Time) vs. the emittance ratio at 10 mA bunch current for both cases. The difference is very small (few %).

BLT changes as the inverse of the bunch current at fixed coupling. Touschek contribution to the emittance and energy spread is negligible. At the nominal current per bunch (15mA) and coupling (0.5%) the beam lifetime is of the order of 1000 sec.

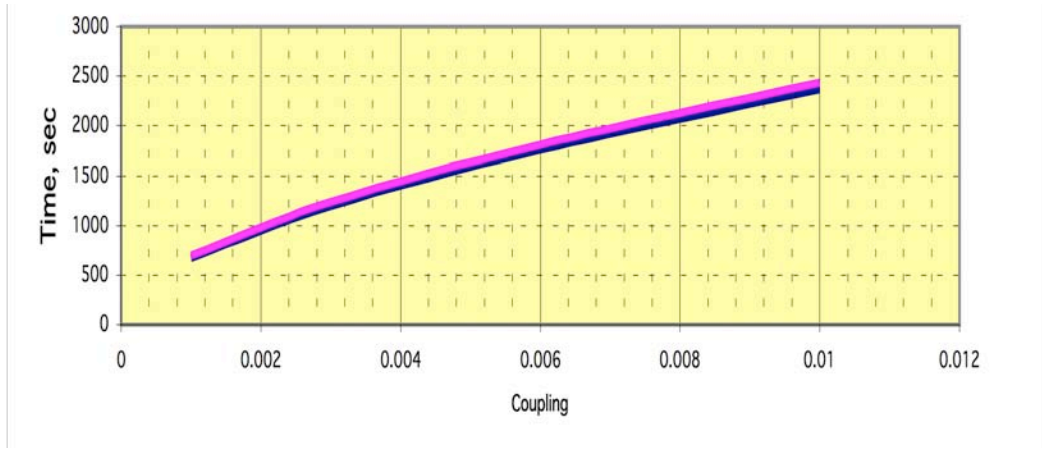


Figure 14 – Beam Life Time vs. emittance coupling at 10 mA bunch current.

Touschek background

Beam induced backgrounds will be dominated by Touschek scattering, as it is now for DAΦNE. Machine optics and vacuum chamber are designed to minimize losses as much as possible, especially at the Interaction Region (IR). Collimators are required upstream the Interaction Point (IP) to remove errant beam particles away from the detector. Shape and position of collimators must be optimized with simulations. Eventually, a masking system can be incorporated to shield the detector from beam-generated background. All these studies are performed with the same tools used successfully for DAΦNE [29].

Most losses arise from the Touschek scattered particles in dispersive regions, so only these particles are simulated. Touschek scattered particles have a betatron oscillation which is proportional to the dispersion D_x , to the invariant H ($\propto D_x$) and to the relative momentum deviation $\delta p/p$:

$$x = \frac{\delta p}{p} (|D_x| + \sqrt{H\beta}).$$

The H-invariant parameter is defined by the following relation:

$$H = \gamma_x D_x^2 + 2\alpha_x D_x D_x' + \beta_x D_x'^2.$$

The value of the H invariant (see Fig. 15) is for DANAÉ smaller by more than a factor two with respect to the one for DAΦNE, thanks to the fact that the emittance is created by a higher field in the wiggler. This reduces the betatron oscillations of the off-energy particles and, as a consequence, the overall particle losses around the beam pipe. However, since most losses are still at the IR, optics modifications are implemented to reduce this effect. Some examples of the scattered particles trajectories are shown in Fig. 16. They hit the vacuum chamber mainly at the focusing quadrupole QF downstream the IP; two scrapers placed about -8m and -12m upstream the IP can stop them.

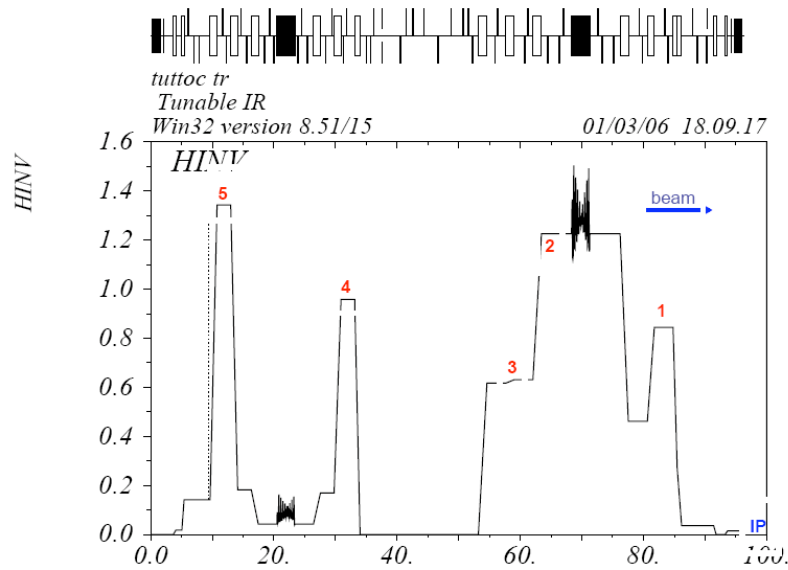


Figure 15 – H-invariant along the ring. In red the regions where Touschek particles are generated.

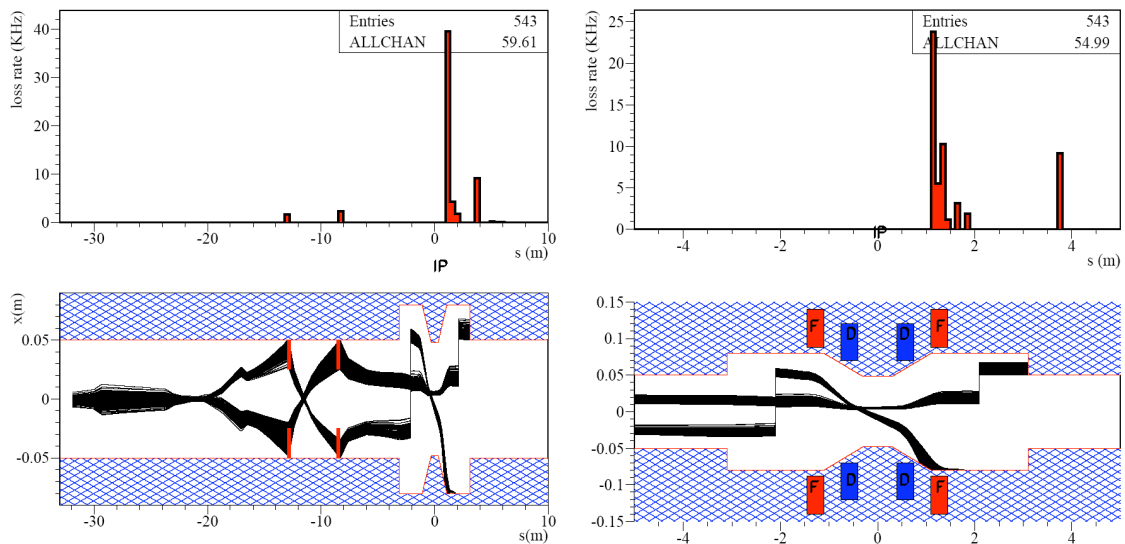


Figure 16 – Trajectories (lower plot) and distribution (upper plot) of particles starting from region 2 upstream the IR and lost at the IR. Left plot is from region 2 to the IR, showing how two collimators can stop all particles which would be otherwise lost at the IR. Right plot shows the IR in more details.

COLLIDER MAIN SYSTEMS

A brief description of the main systems of the DANAE complex follows.

Magnets

Dipoles

The DANAE dipoles are dimensioned with a bending radius longer than the present DAΦNE one, so that the high energy can be reached with normal conducting technology and reasonable magnet gap (43 mm). With such a gap the best solution are the H shaped dipoles. A C shape solution with detachable poles would be very complicate from the mechanical point of view and, since the magnet must ramp up from 0.73 to 1.718 T, the connecting bolts between the various pieces of iron may represent a problem because of eddy currents. The required ramp up/down time must be further investigated, before freezing the magnet design. At this stage only a rough optimization of the magnetic field profile has been done by shimming the pole profile. More detailed 2D and 3D simulations are being accomplished to better evaluate the magnetic field profile. The main parameters of the dipole are listed in Table VII, Fig. 17 shows the Poisson simulation output. All the dipoles have the same bending radius, while there are three different magnetic lengths, as can be seen from the layout shown in Fig. 1.

Table VII – Dipole Magnet Parameter List

Energy	GeV	0.51	1.2
Nominal Field	Tesla	0.73	1.718
Bending Radius	m	2.329	2.329
Magnet gap	mm	43	43
Width	m	0.872	0.872
Height	m	0.683	0.683
Pole width at the gap	m	0.172	0.172
Pole width at the yoke	m	0.252	0.252
Nominal A*turn per pole	A	1650	33100
Turn per pole		64	64
Nominal Current	A	197,66	517.2
Current Density	A/mm ²	0.85	2.22
Copper Conductor	mm*mm	17.4*17.4	17.4*17.4
Cooling Hole Diameter	mm	9.3	9.3

The existing dipole or wiggler power supplies seem to fulfill well the required voltage and current values. However, since they have been designed for steady state operation, a set of measurements must be accomplished to verify the dynamic performances during the current ramp-up to determine if they can effectively be re-used for the upgraded machine. The different types of magnets will have different inductances, therefore only magnets of the same type can be series connected.

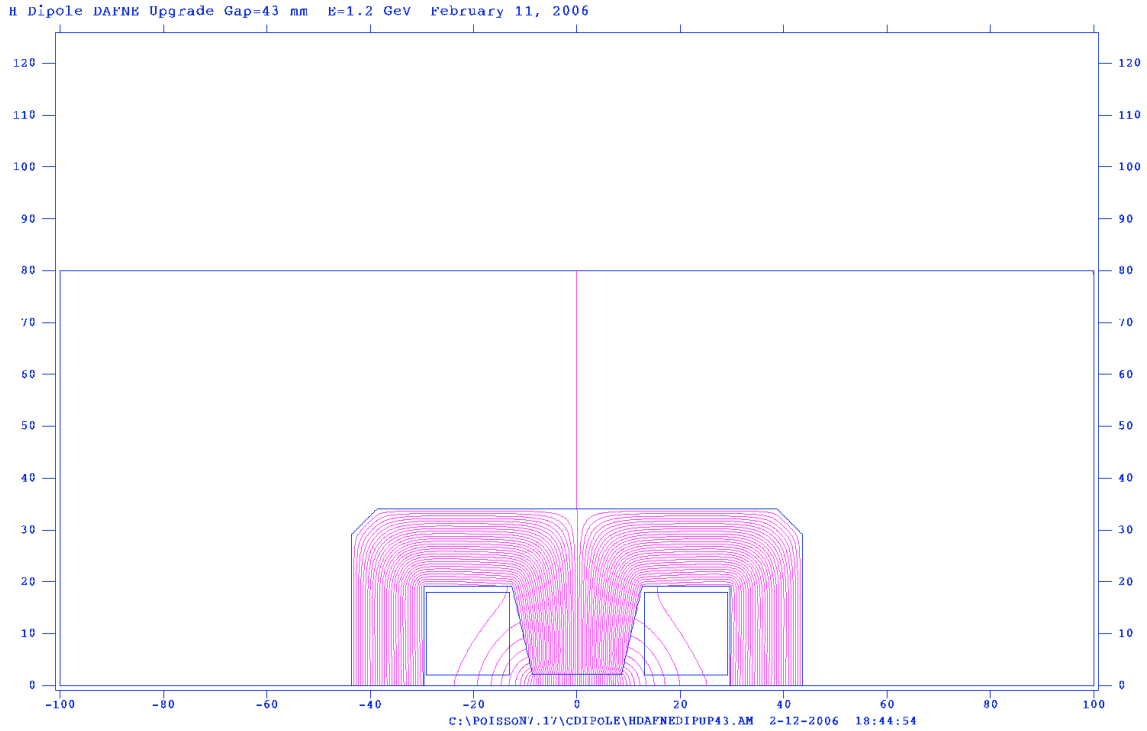


Figure 17 – 1.718 T Dipole Magnet, POISSON simulation output.

Quadrupoles and sextupoles

The total number of quadrupoles in each DANAE ring, not counting the IR magnets, is 46. The maximum integrated gradient is $G_{\max} = 4.5$ T at the highest energy. Figure 18 shows the integrated quadrupole gradients for the two different DANAE regimes of the 46 quadrupoles in each ring.

The number of sextupoles used in the dynamic aperture computation is 15 per ring, but we intend to install some more to ensure flexibility in the future operation. The dynamic aperture has been computed up to now only for the Φ -factory regime, with a peak integrated sextupole gradient of 30 T/m in one family and much lower in all the others.

All DAΦNE quadrupoles, sextupoles, and correctors will be reused in DANAE. Table VIII summarizes the available quadrupoles and sextupoles of the DAΦNE rings with their main characteristics, which fit well the DANAE design.

Table VIII – DAΦNE available quadrupoles and sextupoles.

Type	Total number	Max integrated gradient	Magnetic length (m)
Large aperture quad	8	2.7 T	0.38
Large quad	28	2.7 T	0.29
Small quad	60	4.5 T	0.30
Large sextupole	18	26 T/m	0.15
Small sextupole	14	22 T/m	0.1

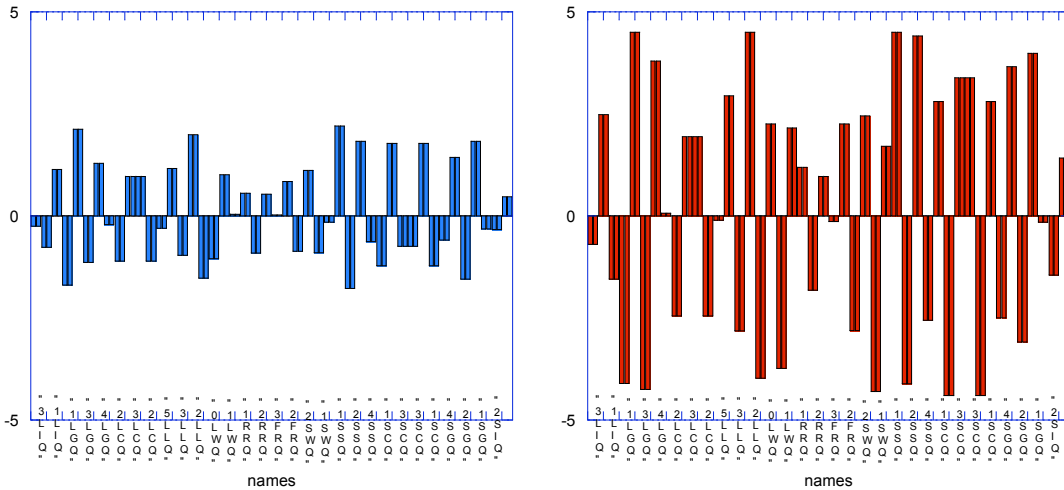


Figure 18 – Integrated gradient (T) for the Φ -factory (left plot) and the maximum energy operation (right plot) for the 46 quadrupoles in each ring.

Wigglers

Two wigglers per ring are used in DANAE for damping and emittance tuning. Their preliminary design, developed in BINP, is described here.

Wiggler magnetic system

The superconducting damping wiggler consists of 19 dipole bending magnets with field amplitude of 4 Tesla. Superconducting windings are made from Cu/Nb-Ti wires, which are placed inside a liquid helium vessel 4.2 °K during normal operation. A superconducting NbTi wire with lacquer insulation is used for the wiggler coils. The main parameters of the magnet are presented in Table IX.

Table IX – Wiggler main parameters

Maximum magnetic field B_{\max}	T	4
Total number of poles		19
Number of main poles		15
Number of poles 3/4		2
Number of poles 1/4		2
Magnetic gap	mm	40
Number of turns at main poles		600
Current in coil	A	314
Total vertical beam stay clear	mm	20
Total horizontal beam stay clear	mm	85
Wire diameter with/without insulation	mm	0.91/0.85
Ratio of NbTi : Cu		0.43
Number of filaments		312
Critical current at 7 Tesla	A	380

Two shield screens used to reduce the irradiation heat flux from outside surround the inner liquid helium vessel. The temperature on the outside shield screen is about 60 °K, on the inner 20 °K. There is vacuum insulation between the helium vessel and the 20 °K screen as well as between both screens and the 60 °K shield and an external warm stainless steel vessel to reduce the heat flux. The walls of the helium vessel face flanges with special stainless steel projections support the magnet. The vessel is hanged with four Kevlar strips connected to the external cryostat vessel. These strips pass through the external vessel walls and are used for precise alignment of the magnet. The wiggler vacuum chamber for the beam is a part of the liquid helium vessel and its temperature is 4.2 °K. To prevent liquid helium consumption due to beam heating a copper absorber is inserted into the vacuum chamber and is kept at 20 °K by two coolers.

Current lead block

Current leads blocks (see Fig. 20) are used to supply current to the magnet. These current leads are the main source of heat in-leak into the liquid helium vessel due to both heat conductivity and joule heat. Each current lead consists of two parts: a normal conducting brass cylinder and a high-temperature superconducting ceramics. One pair of current leads is assembled into one block together with a two stage cooler inside the insulating vacuum of the cryostat. The connection point between normal conducting and superconducting parts of the current leads is kept at 50-65 °K by a first stage of coolers. The lower part of the superconducting part of the current lead is connected with a superconducting Nb-Ti cable and kept below 4.2K by a second stage of the coolers. The power of the second stage is approximately twice more than the in-leak heat power at the lower end of the superconducting current leads and the rest of cooler power is used to cool the liquid helium vessel. This design allows obtaining an average liquid helium consumption less than 0.03 litres/hour and requires liquid helium refilling about once per year at normal operating conditions of the wiggler operation, together with routine maintenance of cooling devices.

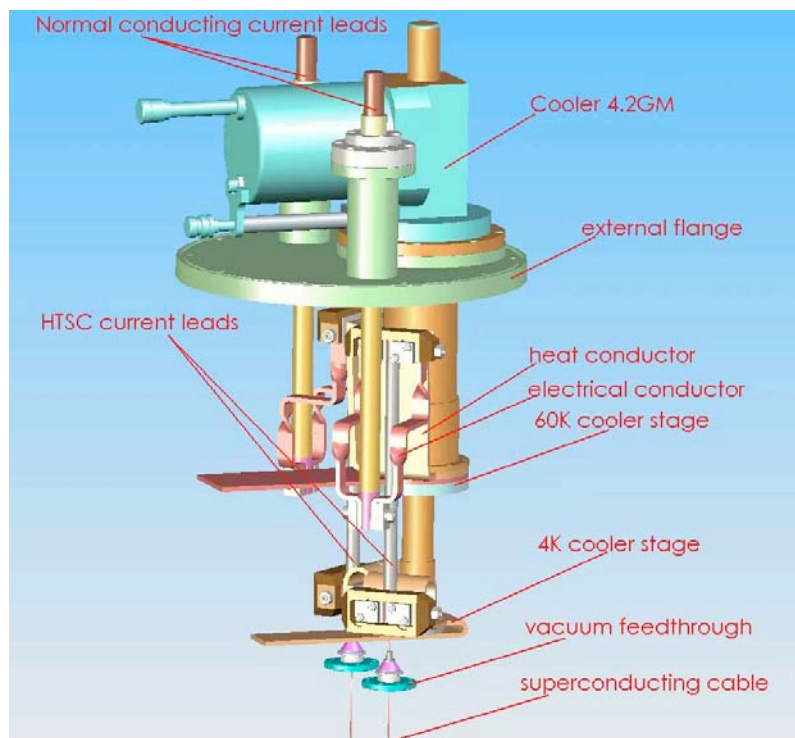


Figure 20 – Current leads block.

